Structure of [Pb(Gly-H)](+) and the Monosolvated Water and Methanol Solvated Species by Infrared Multiple-Photon Dissociation Spectroscopy, Energy-Resolved Collision-Induced Dissoc...

ARTICLE *in* THE JOURNAL OF PHYSICAL CHEMISTRY B · SEPTEMBER 2009

Impact Factor: 3.3 · DOI: 10.1021/jp905654v · Source: PubMed

6 AUTHORS, INCLUDING:

Chad G Atkins
University of British Columbia - Vancouver
8 PUBLICATIONS **95** CITATIONS
SEE PROFILE

Voislav Blagojevic
Vida Holdings Corp.
42 PUBLICATIONS **709** CITATIONS
SEE PROFILE

Diethard K Bohme
York University
422 PUBLICATIONS **8,879** CITATIONS
SEE PROFILE

Travis D Fridgen
Memorial University of Newfoundland
67 PUBLICATIONS **1,151** CITATIONS
SEE PROFILE

Structure of $[Pb(Gly-H)]^+$ and the Monosolvated Water and Methanol Solvated Species by Infrared Multiple-Photon Dissociation Spectroscopy, Energy-Resolved Collision-Induced Dissociation, and Electronic Structure Calculations

Chad G. Atkins,[†] Laura Banu,[‡] Mark Rowsell,[†] Voislav Blagojevic,[‡] Diethard K. Bohme,[‡] and Travis D. Fridgen*[,†]

Department of Chemistry, Memorial University, St. John's, Newfoundland, A1B 3X7 Canada, and Department of Chemistry and Centre for Research in Mass Spectrometry, York University, Toronto, Ontario, M3J 1P3 Canada

Received: June 16, 2009; Revised Manuscript Received: August 23, 2009

Infrared multiple-photon dissociation (IRMPD) spectroscopy, collision-induced dissociation mass spectrometry, and theoretical calculations are combined to provide new insights into the structure and dissociation of lead(II) complexed with the conjugate acid of the amino acid glycine ($[Pb(Gly-H)]^+$) in the presence and absence of solvent. Unexpectedly, these experiments show the main site of lead(II) coordination to be the deprotonated amino group of glycine, with additional coordination to the carbonyl group. In such a structure lead(II) can act as an effective conduit for proton/hydrogen shifts, making H_2O loss competitive with that of CO in the $[Pb(Gly-H)]^+$ complex and leading to solvent deprotonation and formation of $[PbOR(Gly)]^+$ ($R = H, CH_3$) ions when solvent is present in the complex. The structural assignments based on IRMPD spectroscopy are complemented with isotopic labeling experiments ($H_2{}^{18}O$) and experiments done on the ethyl ester of glycine.

1. Introduction

Recently, metal ions have captured the interest of researchers for a broad range of applications in gas-phase chemistry. For example, complexation with aromatic groups has provided a more complete picture of cation$-\pi$ interactions.[1−3] In metal ion complexes of amino acids, the size of the metal cation has been found to influence the propensity for amino acids to adopt zwitterionic structures.[4−15] For example, glycine complexed with Li^+, Na^+, or Be^{2+} adopts a charge solvated structure, whereas K^+, Cu^{2+}, Mg^{2+}, Ca^{2+}, Sr^{2+}, and Ba^{2+} promote a zwitterionic structure.[5,16−19]

One of the more intriguing avenues of gas-phase research involves the development of a detailed picture of how biological systems fundamentally interact. Metal ions are known to play a role in the formation of certain peptides,[20] and obtaining a quantitative scale for their binding energies to small biological molecules is desirable.[21] However, unlike the alkali and alkaline earth metals which have been the focus in the majority of studies referenced above, human exposure to certain heavy metals (Pb, Cd, TI, Hg, etc.) and their respective ionic forms have been known to lead to adverse chemical responses within cells. The degree of toxicity typically depends on how efficiently the heavy metal ion competes for binding sites on proteins and peptides.[22] Acquiring structural information about fundamental interactions between toxic ions and simple biological building blocks can pave the way for modeling the actual physiological response by the larger systems which would be responsible for detoxification.

The tripeptide glutathione (γ-Glu-Cys-Gly, GSH) is well-known to be responsible for detoxification, due to its large concentration within the cell and its ability to chelate metals.[23] Attempts to understand such a process have been undertaken in the past through various means such as NMR[24] and pulse polarography.[25] Burford, Eelman, and LeBlanc[26] used electrospray mass spectrometry to examine the complexes of various heavy metal cations (Pb^{2+}, Cd^{2+}, Hg^{2+}, TI^+, Bi^{3+}) with all 20 standard amino acids as well as homocysteine. The mass spectra revealed that, in most cases, the most abundant complexes for the dication systems involved the heavy metal ions bound to the conjugate base of the amino acid, $(MAa-H)^+$ (M = metal, Aa = amino acid, H = hydrogen). Higher order complexes involving multiple amino acids and metal ions were also identified. Later they expanded upon this work to examine complexes of the same metal ions with glutathione.[27] Collision-induced dissociation (CID) experiments on the complexes showed no neutral fragments containing sulfur, suggesting the importance of cysteine's sulfur atom in chelating the metal species. With these types of experiments, though, it is not possible to provide a more definitive structural characterization.

Many experimental and theoretical approaches have been utilized to study the structures of amino acids when complexed with a metal ion. One of the most recent approaches involves the coupling of a mass spectrometer to a broadly tunable infrared (IR) source for the observation of IR-induced dissociation. As the absorption of multiple photons is necessary for the dissociation to occur, a so-called infrared multiple-photon dissociation (IRMPD) "consequence" spectrum is produced, which has been shown in most cases to correlate well with absorption spectra obtained from theoretical calculations.[28] The radiation sources utilized for this experimental approach include the free electron lasers (FEL) of FELIX[29] and CLIO,[30] and groups have also starting taking advantage of a tabletop OPO/OPA laser setup.[9,19,31−34]

CID, another technique used largely for structural investigations, employs two stages of mass analysis combined in one experiment. In this method a selected precursor ion, upon dissociation by collisions with an inert gas, produces a product ion spectrum in which all fragment ions are derived from the selected precursor ion. Applying this technique, Ohanessian and

* To whom correspondence should be addressed. E-mail: tfridgen@mun.ca.
[†] Memorial University.
[‡] York University.

10.1021/jp905654v CCC: $40.75
Published on Web 09/21/2009

co-workers, for example, have been able to elucidate structures of solvated zinc(II) complexes with carboxylic acids[35] and glycine.[36]

The history of lead derivatives as antiknocking agents in gasoline makes the lead dication an interesting prospect for study; understanding the Pb^{2+} ion interacting with amino acids may lead to rationalizing the effect of its contamination and exposure. Analytical chemists have investigated the ion through various means.[37,38] Here we will provide our gas-phase energy-resolved CID and IRMPD spectroscopy studies on $[Pb(Gly-H)]^+$. Comparisons will be drawn to theoretical spectra with the intention of elucidating intrinsic structural features of these ions. Also included is a study of the structure of the water and methanol solvated $[Pb(Gly-H)]^+$ complexes, $[Pb(Gly-H)H_2O]^+$ and $[Pb(Gly-H)CH_3OH]^+$.

2. Methods

2.1. Experimental Section. ***2.1.1. IRMPD Spectroscopy.*** Ions were electrosprayed from solutions containing approximately 1 mM glycine (Sigma Aldrich) and 1 mM lead nitrate in a 50/50 mixture of 18 MΩ water (Millipore) and methanol using the Apollo II ion source on a Bruker Apex Qe70 Fourier transform ion cyclotron resonance (FTICR) mass spectrometer. Flow rates were typically 100 μL h^{-1}. Ions were initially mass selected in the quadrupole mass filter prior to accumulation in a hexapole trap for 1−2 s and then transferred to the ICR cell where they were irradiated with tunable infrared radiation from an optical parametric oscillator (OPO) for 2−7 s at each wavelength in 1 cm^{-1} intervals.

The OPO laser system/FTICR spectrometer setup will be discussed thoroughly in a forthcoming paper. A brief description will be provided here. The potassium titanyl phosphate (KTP) crystal of the OPO laser (Euroscan, Belgium) was pumped with the fundamental line (1064 nm) from a Brilliant B Nd:YAG laser (Big Sky Laser) with 6 ns pulses at 10 Hz and an output of 850 mJ. The output of the OPO has a 2 cm^{-1} bandwidth. The OPO laser radiation entered the vacuum chamber through a BaF_2 window, and the entire laser path from the laser to the ICR cell, including the bore of the magnet, was purged with dry CO_2-free air and dry N_2. The wavelength of the laser was scanned in 1 cm^{-1} steps, and 2 mass spectra were averaged per wavelength.

For the IRMPD experiments, ions were solvated according to the method developed previously.[39] Briefly, a second transfer line was directed into the hexapole accumulation cell. The first one is for argon collision gas, and the second is a vapor inlet line. The argon flow was typically minimized, while vapor from the liquid was flowing. Either water, methanol, or ^{18}O-labeled water was degassed by three freeze−pump−thaw cycles. The pressure in the hexapole accumulation cell is estimated to be about 10^{-2} mbar, but the microvalve between the liquid and the accumulation cell was opened slowly to effect almost complete single solvation of the selected ion.

2.1.2. Energy-Resolved MS−MS. Experiments were performed using a MDS SCIEX API 2000 triple quadrupole mass spectrometer with a TurboIonSpray ion source. Equimolar solutions of lead derived from lead nitrate (BDH) and glycine (Aldrich) were prepared in methanol or in water (100 μM each). Solutions were introduced directly into the electrospray source, at a typical flow rate of 3 μL min^{-1} and electrospray voltage of 5500 V.

The relative stabilities of different parent and product ions were evaluated by recording breakdown dissociation profiles under multiple collision conditions (nitrogen collision gas, pressure approx 2 mTorr) using the multiple reaction monitoring (MRM) scan mode with laboratory collision voltages between 0 and 100 V. Relative ion intensities were plotted as a function of collision voltage, and the steepest part of the intensity curve was extrapolated to zero by linear regression, with onset voltage represented by the intercept. The final values reported here are averages of at least three individual measurements, represented in the center of mass reference frame (E_{CM}). The uncertainty of the measured onset energy was estimated to be up to ±10%.

2.2. Computations. All calculations were done using the Gaussian 03 software bundle.[40] Geometry optimizations and harmonic vibrational frequency calculations were performed using the B3LYP density functional theory. For Pb, the LANL2DZ basis set and relativistic core potential were used,[41] while the 6-31+G(d,p) basis set was used for all other atoms. Geometries and thermal corrections to the thermochemical data as well as entropies were extracted from this DFT calculation. Single point energy calculations were then performed on all optimized structures using the MP2 level of theory, with the same basis set and core potential for Pb and the larger 6-311++G(2d,2p) basis set for all other atoms. The energies derived by this method are abbreviated as MP2/6-311++G(2d,2p)//B3LYP/6-31+G(d,p), but one should keep in mind that the LANL2DZ basis set and core potential were used for Pb in all calculations. Computed harmonic frequencies were scaled by a factor of 0.955[42] and convoluted with a Lorentzian profile having 10 cm^{-1} full width at half-maximum. The reported enthalpies and 298 K free energy differences are reported relative to the lowest-energy structures.

Transition state structures were verified by the presence of one imaginary frequency which corresponded to the reaction coordinate. Intrinsic reaction coordinate calculations were also performed to verify the reactant and product from the transition state.

3. Results and Discussion

3.1. IRMPD Spectroscopy. The combination of IR radiation sources with mass spectrometry has provided researchers with a significant tool capable of elucidating intrinsic structural information regarding gas-phase ions. In IRMPD, once the impinging IR radiation is in resonance with a vibrational mode of the isolated ion, it becomes energized through absorption of a photon. Rapid intramolecular vibrational energy redistribution (IVR) to other vibrational modes occurs, allowing the absorption of another photon exciting the same mode.[32−34] As this process continues, the internal energy of the ion surpasses the threshold for dissociation and dissociation is observed.

3.1.1. $[Pb(Gly-H)H_2O]^+$. Initially, our attempts at obtaining the IRMPD spectrum of bare $[PbGly-H]^+$ were unsuccessful, presumably because the lowest-energy dissociation threshold was too high (see below) so that the IRMPD process was not efficient enough to observe. Therefore, we added water to $[PbGly-H]^+$ producing $[Pb(Gly-H)H_2O]^+$, which was found to undergo IRMPD when the laser was tuned to be resonant with a vibrational mode. The only dissociation product of this IRMPD process was a loss of neutral water. The experimental IRMPD spectrum for the $[Pb(Gly-H)H_2O]^+$ in the 3200−3800 cm^{-1} region is shown at the top of Figure 1 and will be compared to the theoretical IR spectra after discussing plausible structures.

The spectrum of $[Pb(Gly-H)]H_2O^+$ in Figure 1 has three prominent features, two strong absorptions at 3661 and 3550 cm^{-1} and a weaker absorption in the NH stretching region at 3365 cm^{-1}. Initially it was predicted that the structure of

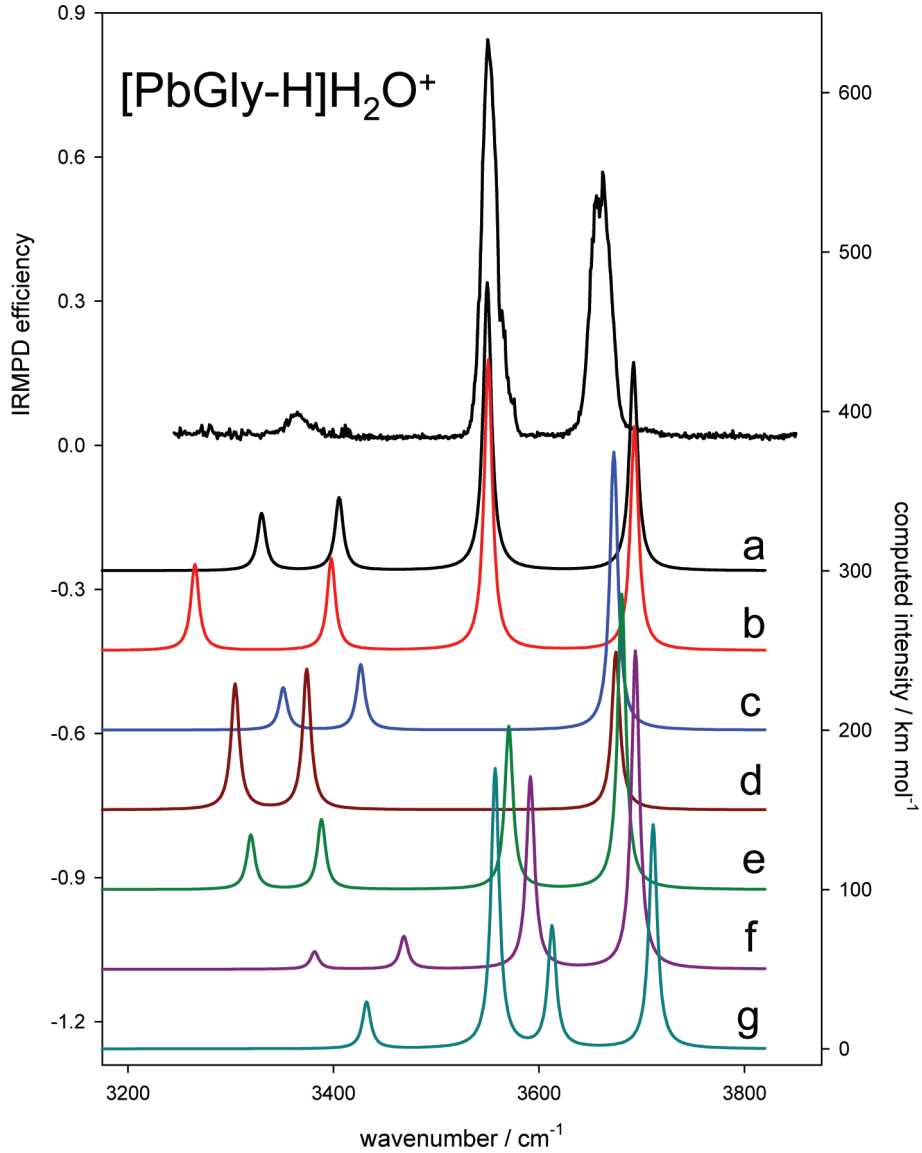

Figure 1. IRMPD spectrum of [Pb(Gly-H)H_2O]$^+$ (top trace) and the B3LYP/6-31+G(d,p) computed spectra for seven isomers. See Figure 3 for corresponding structures.

SCHEME 1: [Pb(Gly-H)H_2O]$^+$ Structures

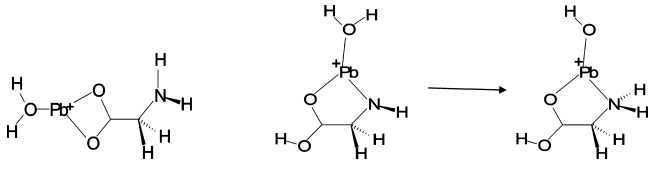

[Pb(Gly-H)H_2O]$^+$ resembles **1** in Scheme 1, where Pb^{2+} has been ligated by zwitterionic glycine which has also lost a proton from the $-NH_3^+$ group. Water would conceivably be bound to Pb^{2+} as well. The positions of the two strong bands are quite interesting and provide telltale signs of the structure which is inconsistent with **1** in Scheme 1. Previous spectroscopic work on the sodium ion- and proton-bound dimers of glycine[19] determined that the O−H stretching vibrations of the carboxylic acid groups are at 3555 and 3569 cm^{-1}, respectively. Similarly, the O−H stretch of canonical matrix isolated glycine is at 3577 cm^{-1}.[43] Furthermore, a matrix isolation study of $Pb(OH)_2$ in solid Ar[44] found the PbO−H stretch to be located at 3640 cm^{-1}. Finally, if water were intact on the ion, two bands associated with the symmetric and asymmetric O−H stretch would be expected, probably slightly red-shifted from ∼3660 and ∼3760 cm^{-1}, respectively. For example, the asymmetric and symmetric stretching vibrations of water complexed to Li^+ in Li^+-bound dimers of thymine and uracil occur at ∼3730 and 3650 cm^{-1}.[45] While theory sometimes guides the peak assignments, this simple group frequency analysis of the experimental data suggests a structure. The similarities of these previous assignments with the band positions observed in the spectrum of [Pb(Gly-H)H_2O]$^+$ (Figure 1) indicated a structure similar to **3** in Scheme 1. An initial entrance channel complex in the reaction of H_2O with [Pb(Gly-H)]$^+$ (**2** in Scheme 1) transfers a proton from water to the amino acid nitrogen.

One implication of this hypothesis on the structure of [Pb(Gly-H)H_2O]$^+$ is that bare [Pb(Gly-H)]$^+$ is nonzwitterionic and the net proton loss from the amino acid is from the N-group rather than from the carboxylic acid group. In other words, the carboxylic acid group is not deprotonated. Calculations were therefore done on various structures of [Pb(Gly-H)]$^+$, and the four lowest-energy structures are displayed in Figure 2. The lowest-energy structure based on these MP2/6-311++G(2d,2p)//B3LYP/6-31+G(d,p) calculations is **i**, in which the proton has been lost from N and still remains on the carboxylic acid group.

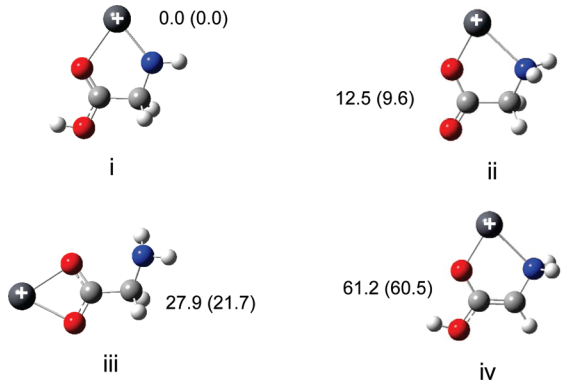

Figure 2. Computed structures for the four lowest-energy isomers of $[Pb(Gly\text{-}H)]^+$ along with the relative enthalpies (kJ mol^{-1}) and 298 K entropies (kJ mol^{-1}) in parentheses.

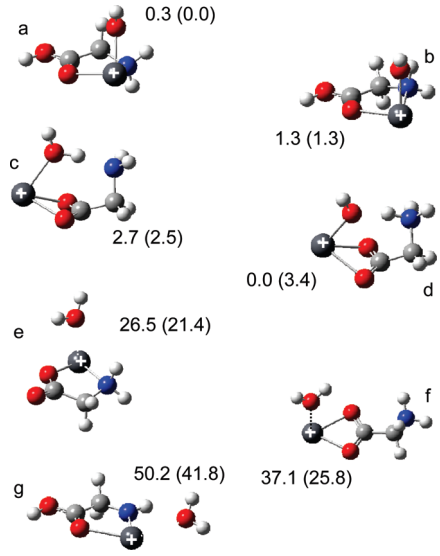

Figure 3. Computed structures for the seven isomers of $[Pb(Gly\text{-}H)H_2O]^+$ along with the relative enthalpies (kJ mol^{-1}) and 298 K entropies (kJ mol^{-1}) in parentheses.

Interestingly, the structure that was initially hypothesized to be the most favorable, **iii**, is the third lowest in energy. The highest energy isomer is **iv**, where the proton has been lost from the methylene group. Note that the spectroscopic data clearly suggested that the structures such as **i** and **iv** needed to be attempted.

From these new theoretical data, calculations were performed on a number of these structures where water was attached as well. The results of these calculations are presented in Figure 3. Although **a**, **b**, **c**, and **d** are all very similar in energy, only the conformers **a** and **b** are structures which could stem from **i** in Figure 2 without extensive hydrogen atom shift isomerization. Structure **g** is also possible, stemming from **i**, and is the entrance channel complex formed upon reaction of neutral water with $[Pb(Gly\text{-}H)]^+$. It is significantly higher in energy, and the energy barrier for isomerization to structure **b** is only about 10 kJ mol^{-1} (see Figure 4). Structures **c**, **d**, and **f** stem from **iii** in Figure 2, the first two of which are strongly stabilized by intramolecular hydrogen bonding interactions.

In Figure 1 the computed IR spectra for **a**−**g** are compared to the experimental IRMPD spectrum of $[Pb(Gly\text{-}H)H_2O]^+$. The predicted spectra for structures **a** and **b** match well with the IRMPD spectrum, but spectroscopically structures **c** and **d** cannot be ruled out as being present simply because they do not have a band predicted to be at 3550 cm^{-1} where a band is

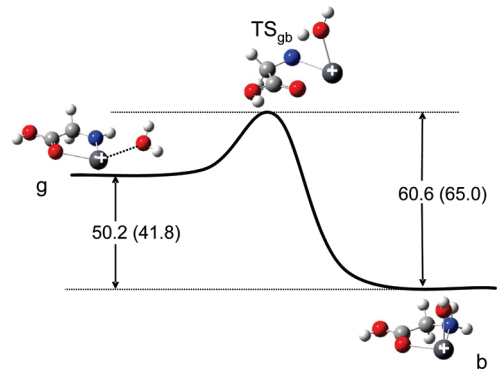

Figure 4. Proton-transfer isomerization profile between structures **g** and **b** of $[Pb(Gly\text{-}H)H_2O]^+$.

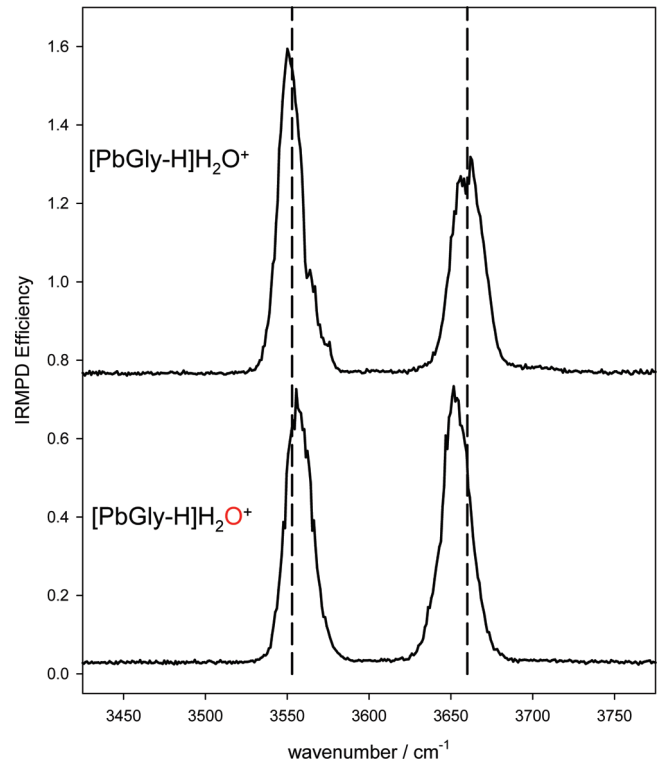

Figure 5. IRMPD spectrum of $H_2{}^{16}O$ (top trace) and $H_2{}^{18}O$ (bottom trace) labeled $[Pb(Gly\text{-}H)H_2O]^+$.

observed in the experimental spectrum. The remaining experimental features compare favorably with the other predicted bands for **c** and **d**. All that can be concluded spectroscopically is that structures **c** and **d** are, at most, minor contributors. Structures **c** and **d** cannot be ruled out based upon their computed energies either. However, one can surmise that since **i** is the lowest-energy $[Pb(Gly\text{-}H)]^+$ isomer, then the addition of a water molecule in the gas phase should initially give **g** and then a mixture of **a** and **b**. To obtain structures such as **c** and **d**, many rearrangements, including a proton shift and Pb^{2+} ion shift, with significant energy barriers would not likely occur rapidly. Structures **e** and **f** cannot be ruled out by comparing the experimental and computed spectra. An IRMPD spectrum of $[Pb(Gly\text{-}H)H_2O]^+$ where the water was labeled with ^{18}O is shown in Figure 5. If the two intense bands in the IRMPD spectrum of $[Pb(Gly\text{-}H)H_2O]^+$ were due to the symmetric and asymmetric O−H stretching absorptions of the water, as in structures **e** and **f**, then both bands would be expected to shift to lower wavenumber position, by approximately 10 cm^{-1}. However, the only one that shows a red shift is the 3661 cm^{-1}

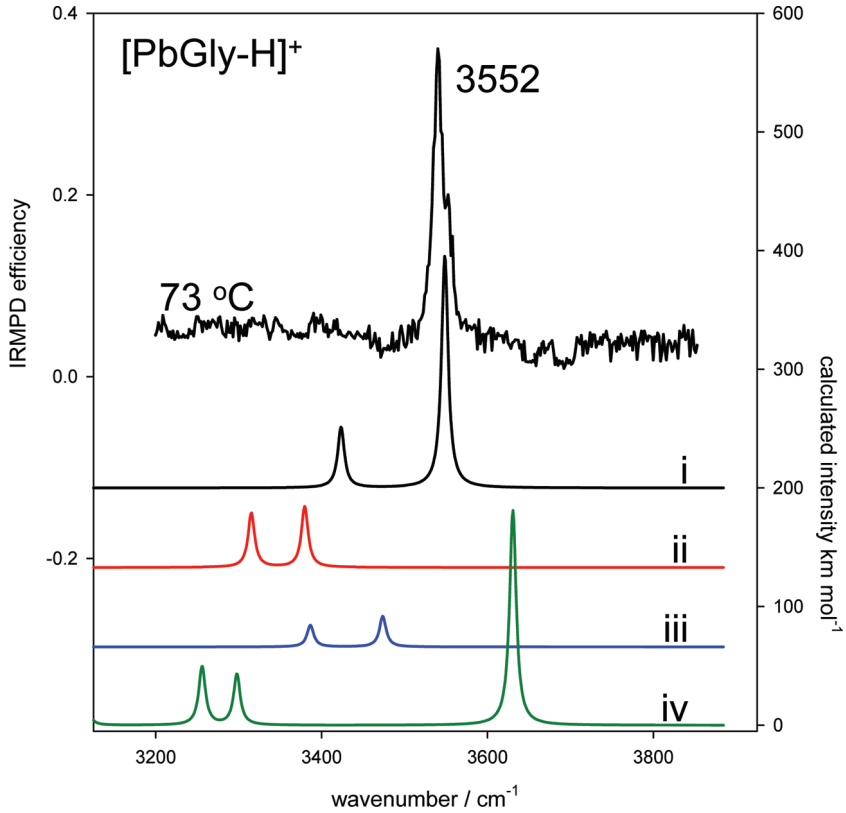

Figure 6. IRMPD spectrum of [Pb(Gly-H)]$^+$ at 73 °C compared with the computed spectra for the four lowest energy isomers (see Figure 2 for structures).

band, as expected if the structure of the observed ion were as represented by structures **a** and **b**.

3.1.2. [Pb(Gly-H)]$^+$. By heating of the vacuum chamber housing the ICR cell with a heating jacket (which is cooled on the outside to protect the magnet), the internal ICR cell temperature was increased to 73 °C. At this temperature the internal energy of [Pb(Gly-H)]$^+$ was high enough to observe IRMPD and the predominant fragmentation pathway observed upon absorption of the OPO laser was CO loss, with a very small amount of H_2O loss (9% of CO loss). The IRMPD spectrum is shown in Figure 6 along with the IR absorption spectra predicted for the four structures in Figure 2. The band observed at 3552 cm^{-1}, in virtually the same position as that assigned to the carboxylic acid O−H stretch for [Pb(Gly-H)H_2O]$^+$, is still present in the absence of water, consistent with there being a −COOH group in the complex and the proton being lost from N in [Pb(Gly-H)]$^+$ as in structure **i**. The computed spectrum for this lowest energy structure, **i**, is also the best match to the experimental infrared spectrum confirming this structure. This is also consistent with the conclusion that [Pb(Gly-H)H_2O]$^+$ is most likely structures **a** and **b** and not **c**−**f**. Experiments of Rogalewicz, Hoppilliard, and Ohanessian[36] on [Zn(Gly−H)]$^+$ also predict that glycine is preferentially deprotontated at N in this complex even though deprotonation at N is some 200 kJ mol^{-1} higher in energy.[46] The present work is the first experimental evidence for deprotonation at N of these complexes of metal cations and deprotonated amino acids.

3.1.3. [Pb(Gly-H)CH_3OH]$^+$. Methanol was complexed to [Pb(Gly-H)]$^+$ in the accumulation cell producing [Pb(Gly-H)CH_3OH]$^+$. Upon absorption of the infrared laser, the only fragmentation pathway observed was loss of methanol. The IRMPD spectrum is shown in Figure 7. The band at 3552 cm^{-1} is present, indicative of a carboxylic acid O−H stretch. Since it is anticipated that there would be a transfer of a proton from the hydroxyl group of methanol to N in the complex, there would be a $PbOCH_3$ group rather than a PbOH group. The absence of a strong band ∼3660 cm^{-1} as there was in [Pb(Gly-H)H_2O]$^+$ is expected. Comparing the experimental spectrum with the computed spectra, it is evident that structures **B** and **C** could not be the only species present. Even though structure **B** is the lowest energy structure, it would only be formed via extensive rearrangement from structure **i** involving a proton transfer from the carboxylic acid end to the NH group. Solvation of [Pb(Gly-H)]$^+$, structure **i**, would initially produce **D** and would be expected to rearrange to structure **A** through a transition state which is similar to that shown in Figure 4 for the H_2O solvated species. The energy barrier for this proton-shift isomerization is also calculated to be similar, ∼10 kJ mol^{-1}.

There is a diffuse band centered at 3648 cm^{-1} which may suggest that methanol is not dissociated or not completely dissociated and that there is at least a mixture of structures **A** and **D**. The diffuseness of the 3648 cm^{-1} band is explained by some hydrogen bonding interaction between the absorbing O−H group on methanol with the nitrogen atom of glycine as seen in Figure 7. This 3648 cm^{-1} band is most likely explained by the presence of structure **D**.

3.1.4. Ethyl Ester, [Pb(GlyOOEt−H)H_2O]$^+$. The complex between Pb^{2+} and the conjugate base of glycine ethyl ester, [Pb(GlyOOEt−H)]$^+$, was electrosprayed and singly hydrated in the accumulation cell. Upon absorption of the infrared laser, [Pb(GlyOOEt−H)H_2O]$^+$ was observed to lose water as the sole dissociation process. The spectrum of [Pb(GlyOOEt−H)H_2O]$^+$ is shown in Figure 8 and compared with the spectra of the other species previously presented in this paper. There are two important observations made by comparing this spectrum to the others. First, the band observed in the spectra of the other species around 3550 cm^{-1} and assigned to the −COO−H stretch is not present in the [Pb(GlyOOEt−H)H_2O]$^+$ as expected since the

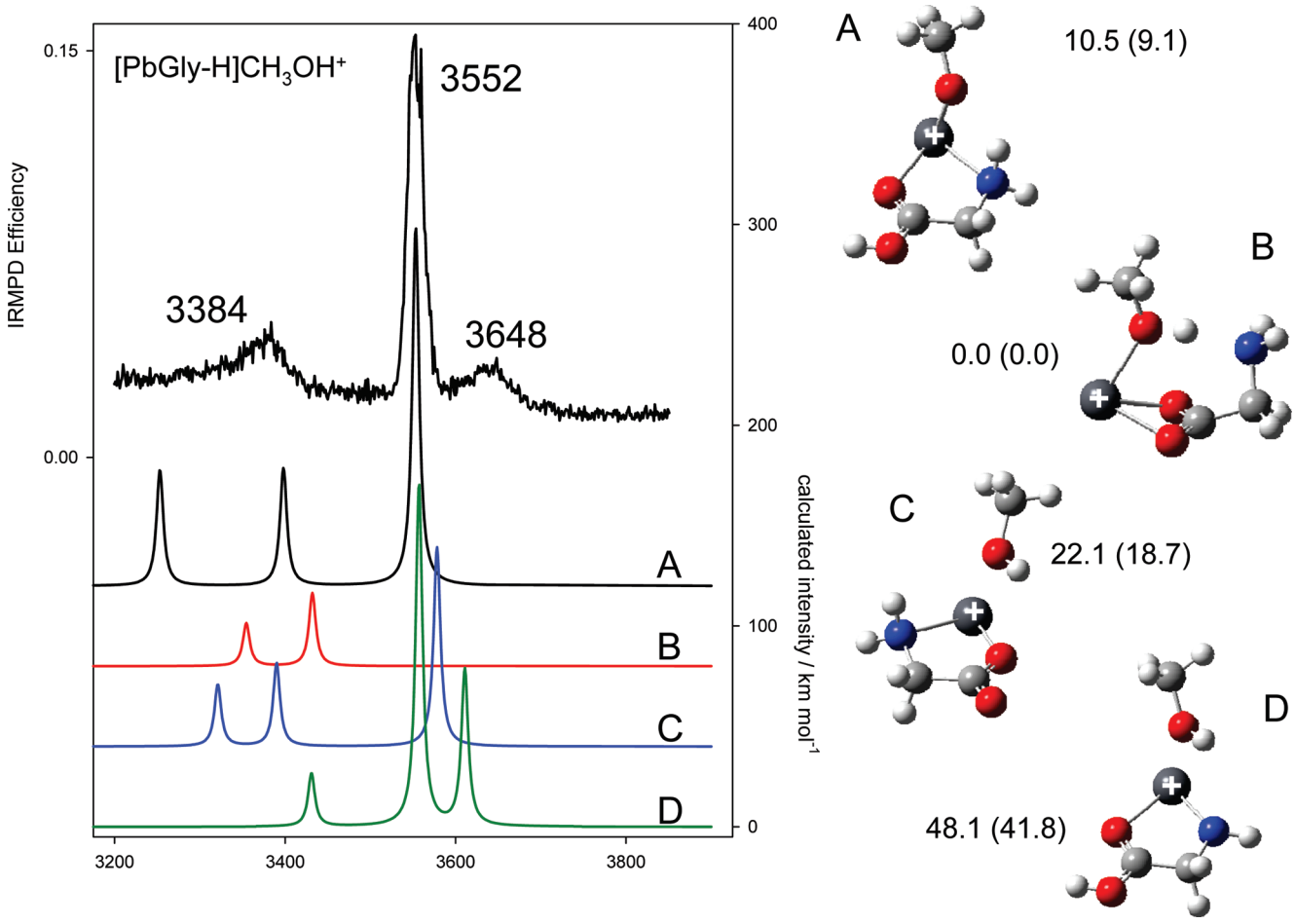

Figure 7. IRMPD spectrum of $[Pb(Gly\text{-}H)CH_3OH]^+$ compared with the computed spectra for four isomeric structures.

−H has been replaced by $-CH_2CH_3$ (or probably more precisely the −OH has been replaced by $-OCH_2CH_3$). This is consistent with our assignment of the 3550 cm^{-1} band to the −COO−H stretch. Second, the band at about 3660, also present in the spectrum of $[Pb(Gly\text{-}H)H_2O]^+$, confirms the assignment of this band to the PbO−H stretching absorption.

3.2. CID Results. In Figure 9 are the MRM profiles recorded for the dissociation of the $[Pb(Gly\text{-}H)S]^+$ complex ions (S = solvent) generated in pure water and in pure methanol solutions. Both primary and higher order collision-induced dissociations were observed. The onset voltages for the dissociation of product ions are listed in Table 1, and these provide insight into the sequence of dissociation. The higher onset energies from the solvated ions are expected because of the extra energy required for desolvation. The increasing differences in the onsets with increasing onset energies that are evident in Table 1 can be attributed to increasing excess energy of the collisions being stored in the solvent molecules. In effect the solvent molecule acts to dampen the collisions, and the extent of dampening will increase with the collision energy. There are some slight differences in onset energies between ions created in water and methanol that may reflect a larger dampening by methanol, but these are within the error margins of the experiment.

Figure 9 shows that the solvated ions first lose the solvent molecule upon collision according to reaction 1.

$$[Pb(Gly\text{-}H)S]^+ \xrightarrow{CID} [Pb(Gly\text{-}H)]^+ + S \qquad (1)$$

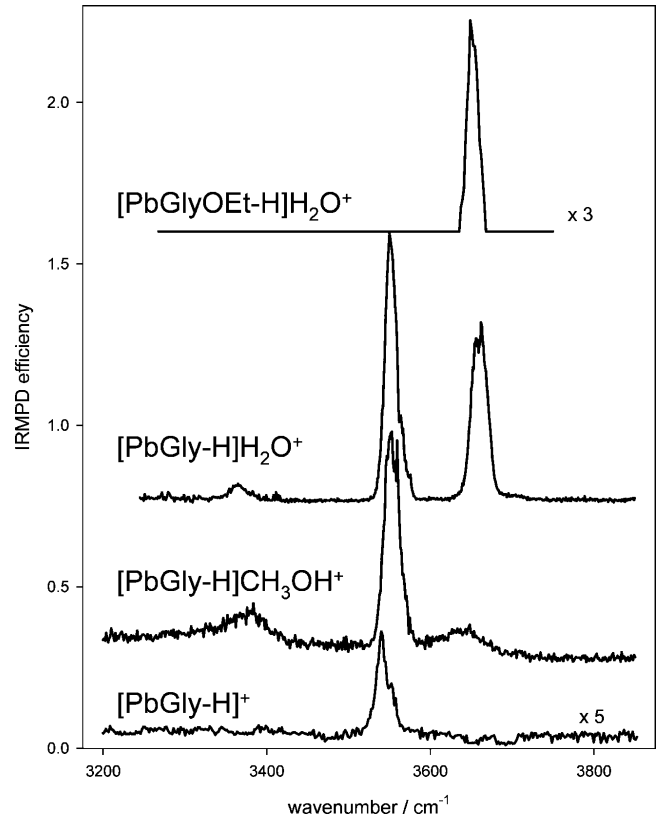

Figure 8. Comparison of the experimental IRMPD spectra of $[Pb(GlyOEt{-}H)H_2O]^+$, $[Pb(Gly\text{-}H)H_2O]^+$, $[Pb(Gly\text{-}H)CH_3OH]^+$, and $[Pb(Gly\text{-}H)]^+$.

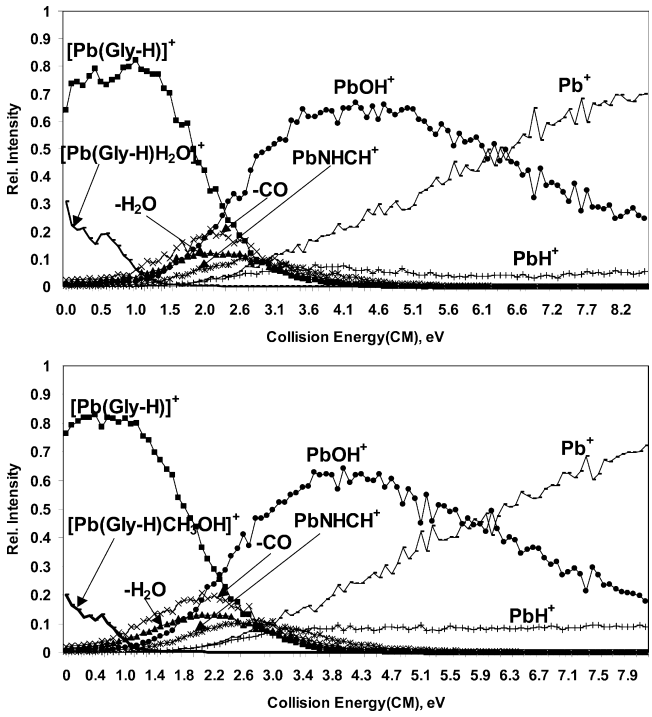

Figure 9. Dissociation profiles obtained for [Pb(Gly-H)S]$^+$ ions, where S is a solvent molecule of water (top) or methanol (bottom).

Two primary covalent bond dissociations are observed following desolvation: the elimination of carbon monoxide, reaction 2, and the elimination of water, reaction 3.

$$[Pb(Gly\text{-}H)]^+ \xrightarrow{CID} [Pb(Gly\text{-}H{-}CO)]^+ + CO \qquad (2)$$

$$[Pb(Gly\text{-}H)]^+ \xrightarrow{CID} [Pb(Gly\text{-}H{-}H_2O)]^+ + H_2O \qquad (3)$$

Further dissociation of the resulting ion [Pb(Gly-H−CO)]$^+$ leads to PbOH$^+$ and then Pb$^+$ according to reaction 4.

$$[Pb(Gly\text{-}H{-}CO)]^+ \xrightarrow{CID} PbOH^+ + NHCH_2 \xrightarrow{CID} Pb^+ + OH \qquad (4)$$

SCHEME 2: Proposed Mechanism for the Dissociation of the (1:1) Lead−Glycine Complex, [Pb(Gly-H)]$^+$

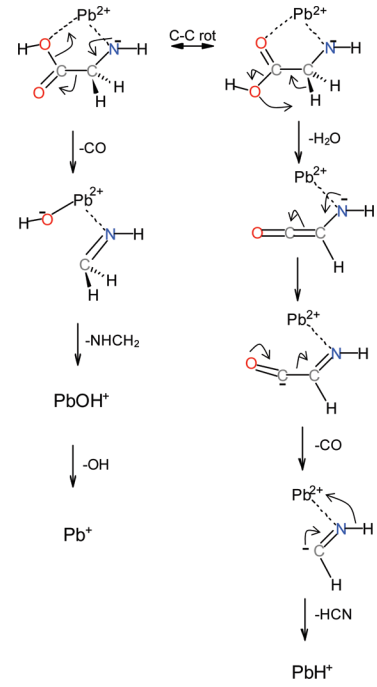

[Pb(Gly-H−H$_2$O)]$^+$ undergoes successive losses of CO and HCN to form PbH$^+$ according to reaction 5.

$$[Pb(Gly\text{-}H_2O)]^+ \xrightarrow{CID} [PbNHCH]^+ + CO \xrightarrow{CID} PbH^+ + HCN \qquad (5)$$

The observed dissociation of the desolvated complex [Pb(Gly-H)]$^+$ can be understood with the mechanism proposed in Scheme 2. The structure of the [Pb(Gly-H)]$^+$ formed initially in the electrospray process is not necessarily reflected in the product ions resulting from the CID experiments since the multicollisional nature of the CID process may lead to isomerization of the [Pb(Gly-H)]$^+$ complex prior to dissociation (see Scheme 2). The CID studies suggest that losses of CO and H$_2$O from [Pb(Gly-H)]$^+$ are relatively isoenergetic processes, while the much softer process of IRMPD on [Pb(Gly-H)]$^+$ shows that CO loss is preferred. The mechanism proposed in Scheme 2 shows both pathways. The initial loss of CO requires an isomerization of **i** to a higher energy structure. While both losses of CO and H$_2$O have similar onset energies, loss of H$_2$O requires the transfer of a hydrogen atom, shown to originate from the

TABLE 1: Onset Energies (CM)[a] for Product Ion Formation Initiated by the Dissociation of [Pb(Gly-H)]$^+$or [Pb(Gly-H)S]$^+$

dissociation channel of [Pb(Gly-H)]$^+$	onset energy (CM), eV			
	solvent: H$_2$O		solvent: MeOH	
	[Pb(Gly-H)H$_2$O]$^+$	[Pb(Gly-H)]$^+$	[Pb(Gly-H)MeOH]$^+$	[Pb(Gly-H)]$^+$
(1) CO loss	0.7 ± 0.1	0.5 ± 0.1	0.6 ± 0.1	0.5 ± 0.1
(2) H$_2$O loss	0.7 ± 0.1	0.5 ± 0.1	0.7 ± 0.1	0.3 ± 0.1
(3) PbNHCH$^+$ formation	1.1 ± 0.1	0.8 ± 0.1	1.1 ± 0.1	0.9 ± 0.1
(4) PbOH$^+$ formation	1.5 ± 0.1	1.0 ± 0.1	1.5 ± 0.1	1.1 ± 0.1
(5) PbH$^+$ formation	1.7 ± 0.1	1.4 ± 0.1	1.7 ± 0.1	1.3 ± 0.1
(6) Pb$^+$ formation	2.1 ± 0.1	1.7 ± 0.1	2.3 ± 0.1	1.6 ± 0.1

[a] Onset energy (CM) = $E_{lab}m_{N2}/(m_{N2} + m_c)$, where E_{lab} is the laboratory collision voltage, m_{N2} is the mass of the collision gas molecules, and m_c is the mass of the complex ion.

methylene group. Although the presence of lead makes the amino hydrogens quite mobile, as shown by the formation of $[PbOH(Gly)]^+$ when $[Pb(Gly\text{-}H)]^+$ is hydrated, the transfer of the last hydrogen from N is not likely. Furthermore, hydrogen transfer from the methylene group necessitates a tight transition state such that at higher collision energies CO loss is kinetically more favorable as seen experimentally.

4. Conclusions

Prior gas-phase work had identified the ion produced when Pb^{2+} is complexed with glycine as being of the form $[Pb(Gly\text{-}H)]^+$.[26] Taking such experimentation one step further, energy-resolved CID and IRMPD spectroscopy in the 3200−3700 cm^{-1} range can be combined to elucidate the actual structures of these species. Using IRMPD spectroscopy, the ability to deduce the structure a posteriori was clearly shown for these systems. The structure of $[Pb(Gly\text{-}H)H_2O]^+$ from the IRMPD experiments has an intact −COOH group meaning that glycine is deprotonated on N. The results of these experiments guided the theoretical calculations which confirmed that the lowest-energy structure was indeed that deduced from experiment. Energy-resolved collision-induced dissociation experiments are analyzed in terms of the structure determined from the IRMPD spectroscopy experiments. Plausible mechanisms of final CID products, PbH^+ and Pb^+, from $[Pb(Gly\text{-}H)]^+$, and in fact from the solvated structures as well, are proposed. Detailed calculations of the potential energy surface for $[Pb(Gly\text{-}H)]^+$ dissociation could help in the mechanistic proposal but are beyond the scope of this work.

Further experimentation is needed on cysteine and glutamic acid with the Pb^{2+} ion in order to proceed onward with attempts to understand the binding of such heavy metal ions with glutathione.

Acknowledgment. T.D.F. wishes to gratefully acknowledge the funding contributions from NSERC, CFI, IRIF (government of Newfoundland), and Memorial University. D.K.B. thanks NSERC, MDS SCIEX, and the Canada Research Chair program for their contributions to this research. The authors wish to thank Yuming Zhao for helpful discussions about the CID mechanism.

References and Notes

(1) Dunbar, R. C. *J. Phys. Chem. A* **2000**, *104*, 8067.
(2) Gapeev, A.; Yang, C.-N.; Klippenstein, S. J.; Dunbar, R. C. *J. Phys. Chem. A* **2000**, *104*, 3246.
(3) Grimm, R. L.; Mangrum, J. B.; Dunbar, R. C. *J. Phys. Chem. A* **2004**, *108*, 10897.
(4) Dunbar, R. C.; Polfer, N. C.; Oomens, J. *J. Am. Chem. Soc.* **2007**, *129*, 14562.
(5) Strittmatter, E. F.; Lemoff, A. S.; Williams, E. R. *J. Phys. Chem. A* **2000**, *104*, 9793.
(6) Bush, M. F.; Oomens, J.; Saykally, R. J.; Williams, E. R. *J. Am. Chem. Soc.* **2008**, *130*, 6463.
(7) Drayss, M. K.; Blunk, D.; Oomens, J.; Schaefer, M. *J. Phys. Chem. A* **2008**, *112*, 11972.
(8) Kapota, C.; Lemaire, J.; Maitre, P.; Ohanessian, G. *J. Am. Chem. Soc.* **2004**, *126*, 1836.
(9) Bush, M. F.; O'Brien, J. T.; Prell, J. S.; Saykally, R. J.; Williams, E. R. *J. Am. Chem. Soc.* **2007**, *129*, 1612.
(10) Bush, M. F.; Oomens, J.; Williams, E. R. *J. Phys. Chem. A* **2009**, *113*, 431.
(11) Forbes, M. W.; Bush, M. F.; Polfer, N. C.; Oomens, J.; Dunbar, R. C.; Williams, E. R.; Jockusch, R. A. *J. Phys. Chem. A* **2007**, *111*, 11759.
(12) O'Brien, J. T.; Prell, J. S.; Steill, J. D.; Oomens, J.; Williams, E. R. *J. Phys. Chem. A* **2008**, *112*, 10823.
(13) Hoyau, S.; Ohanessian, G. *Chem.—Eur. J.* **1998**, *4*, 1561.
(14) Remko, M.; Rode, B. M. *J. Phys. Chem. A* **2006**, *110*, 1960.
(15) Wyttenbach, T.; Witt, M.; Bowers, M. T. *J. Am. Chem. Soc.* **2000**, *122*, 3458.
(16) Bertran, J.; Rodriguez-Santiago, L.; Sodupe, M. *J. Phys. Chem. B* **1999**, *103*, 2310.
(17) Hoyau, S.; Pelicier, J.-P.; Rogalewicz, F.; Hoppilliard, Y.; Ohanessian, G. *Eur. J. Mass Spectrom.* **2001**, *7*, 303.
(18) Wyttenbach, T.; Witt, M.; Bowers, M. T. *Int. J. Mass Spectrom.* **1999**, *182/183*, 243.
(19) Atkins, C. G.; Rajabi, K.; Gillis, E. A. L.; Fridgen, T. D. *J. Phys. Chem. A* **2008**, *112*, 10220.
(20) Rode, B. M. *Peptides* **1999**, *20*, 773.
(21) Hoyau, S.; Norrman, K.; McMahon, T. B.; Ohanessian, G. *J. Am. Chem. Soc.* **1999**, *121*, 8864.
(22) Belcastro, M.; Marino, T.; Russo, N.; Toscano, M. *J. Mass Spectrom.* **2005**, *40*, 300.
(23) Meister, A. *J. Biol. Chem.* **1988**, *263*, 17205.
(24) Fuhr, B. J.; Rabenstein, D. L. *J. Am. Chem. Soc.* **1973**, *95*, 6944.
(25) Cruz, B. H.; Diaz-Cruz, J. M.; Diaz-Cruz, M. S.; Arino, C.; Esteban, M.; Tauler, R. *J. Electroanal. Chem.* **2001**, *516*, 110.
(26) Burford, N.; Eelman, M. D.; LeBlanc, W. G. *Can. J. Chem.* **2004**, *82*, 1254.
(27) Burford, N.; Eelman, M. D.; Groom, K. *J. Inorg. Biochem.* **2005**, *99*, 1992.
(28) Oomens, J.; Tielens, A. G. G. M.; Sartakov, B. G.; von Helden, G. *Astrophys. J.* **2003**, *591*, 968.
(29) Oepts, D.; van der Meer, A. F. G.; van Amersfoort, P. W. *Infrared Phys. Technol.* **1995**, *36*, 297.
(30) Ortega, J. M.; Berset, J. M.; Chaput, R.; Glotin, F.; Humbert, G.; Jaroszynski, D.; Joly, P.; Kergosien, B.; Lesrel, J. *Nucl. Instrum. Methods Phys. Res., Sect. A* **1996**, *375*, 618.
(31) Oh, H.; Breuker, K.; Sze, S. K.; Ge, Y.; Carpenter, B. K.; McLafferty, F. W. *Proc. Natl. Acad. Sci. U.S.A.* **2002**, *99*, 15863.
(32) Eyler, J. R. *Mass Spectrom. Rev.* **2009**, *28*, 448.
(33) Fridgen, T. D. *Mass Spectrom. Rev.* **2009**, *28*, 586.
(34) Polfer, N. C.; Oomens, J. *Mass Spectrom. Rev.* **2009**, *28*, 468.
(35) Rogalewicz, F.; Louazel, G.; Hoppilliard, Y.; Ohanessian, G. *Int. J. Mass Spectrom.* **2003**, *228*, 779.
(36) Rogalewicz, F.; Hoppilliard, Y.; Ohanessian, G. *Int. J. Mass Spectrom.* **2001**, *206*, 45.
(37) Lobinski, R.; Adams, F. C. *Anal. Chim. Acta* **1992**, *262*, 285.
(38) Gorecki, T.; Pawliszyn, J. *Anal. Chem.* **1996**, *68*, 3008.
(39) Rajabi, K.; Easterling, M. L.; Fridgen, T. D. *J. Am. Soc. Mass Spectrom.* **2009**, *20*, 411.
(40) Frisch, M. J.; Trucks, G. W.; Schlegel, H. B.; Scuseria, G. E.; Robb, M. A.; Cheeseman, J. R.; Montgomery, J. A., Jr.; Vreven, T.; Kudin, K. N.; Burant, J. C.; Millam, J. M.; Iyengar, S. S.; Tomasi, J.; Barone, V.; Mennucci, B.; Cossi, M.; Scalmani, G.; Rega, N.; Petersson, G. A.; Nakatsuji, H.; Hada, M.; Ehara, M.; Toyota, K.; Fukuda, R.; Hasegawa, J.; Ishida, M.; Nakajima, T.; Honda, Y.; Kitao, O.; Nakai, H.; Klene, M.; Li, X.; Knox, J. E.; Hratchian, H. P.; Cross, J. B.; Bakken, V.; Adamo, C.; Jaramillo, J.; Gomperts, R.; Stratmann, R. E.; Yazyev, O.; Austin, A. J.; Cammi, R.; Pomelli, C.; Ochterski, J. W.; Ayala, P. Y.; Morokuma, K.; Voth, G. A.; Salvador, P.; Dannenberg, J. J.; Zakrzewski, V. G.; Dapprich, S.; Daniels, A. D.; Strain, M. C.; Farkas, O.; Malick, D. K.; Rabuck, A. D.; Raghavachari, K.; Foresman, J. B.; Ortiz, J. V.; Cui, Q.; Baboul, A. G.; Clifford, S.; Cioslowski, J.; Stefanov, B. B.; Liu, G.; Liashenko, A.; Piskorz, P.; Komaromi, I.; Martin, R. L.; Fox, D. J.; Keith, T.; Al-Laham, M. A.; Peng, C. Y.; Nanayakkara, A.; Challacombe, M.; Gill, P. M. W.; Johnson, B.; Chen, W.; Wong, M. W.; Gonzalez, C.; Pople, J. A. *Gaussian 03*, revision C.02; Gaussian, Inc.: Wallingford, CT, 2004.
(41) Cornard, J. P.; Dangleterre, L.; Lapouge, C. *Chem. Phys. Lett.* **2006**, *419*, 304.
(42) Kamariotis, A.; Boyarkin, O. V.; Mercier, S. R.; Beck, R. D.; Bush, M. F.; Williams, E. R.; Rizzo, T. R. *J. Am. Chem. Soc.* **2006**, *128*, 905.
(43) Linder, R.; Seefeld, K.; Vavra, A.; Kleinermanns, K. *Chem. Phys. Lett.* **2008**, *453*, 1.
(44) Wang, X.; Andrews, L. *J. Phys. Chem. A* **2005**, *109*, 10689.
(45) Gillis, E. A. L.; Rajabi, K.; Fridgen, T. D. *J. Phys. Chem. A* **2009**, *113*, 824.
(46) O'Hair, R. A. J.; Blanksby, S.; Styles, M.; Bowie, J. H. *Int. J. Mass Spectrom.* **1999**, *182/183*, 203.

JP905654V